Infantile-Onset Spinocerebellar Ataxia: MR and CT Findings

Tuula Koskinen, Leena Valanne, Leena M. Ketonen, and Helena Pihko

PURPOSE: To report the MR and CT findings in a hereditary disease, infantile-onset spinocerebellar ataxia (IOSCA). **METHODS:** We studied the brains of 17 patients with infantile-onset spinocerebellar ataxia with CT and/or MR to determine the presence of cerebellar and brain stem atrophy and parenchymal lesions. **RESULTS:** Cerebellar cortical atrophy was seen in 13 patients. The degree of atrophy correlated with increasing age and clinical deterioration. Brain stem atrophy was seen in 8 patients. It was never severe, and the basis pontis was not flattened even in the most severe cases. Hyperintense lesions were noted within the white matter of cerebellum, in the dentate nuclei, and in the middle cerebellar peduncles in 3 patients. The upper cervical cord was seen in 9 patients and showed mild to moderate atrophy in 4. The basal ganglia and cerebral hemispheres were normal, except in 2 patients transient cortical and subcortical lesions developed during episodes of status epilepticus; mild cortical brain atrophy subsequently developed. **CONCLUSION:** The brain MR and CT findings of patients with infantile-onset spinocerebellar ataxia correspond to the neuropathologic entities of cerebellar cortical atrophy, olivopontocerebellar atrophy, and spinocerebellar atrophy. The appearance of the findings followed a uniform time sequence from cerebellar cortical atrophy in the early stage of the disease to olivopontocerebellar atrophy and spinocerebellar atrophy in the later stage. The severity of atrophy correlated with clinical deterioration.

Index terms: Familial conditions; Infants, diseases; Degenerative disease; Brain, diseases; Spine, diseases

AJNR Am J Neuroradiol 16:1427–1433, August 1995

We have recently described a recessively inherited ataxia: infantile-onset spinocerebellar ataxia (IOSCA) (1, 2). The gene defect causing the disease has been located at chromosome 10 (3). The clinical symptoms of IOSCA include ataxia associated with peripheral sensory neuropathy, cerebral symptoms including athetosis and epilepsy, deafness, opthalmoplegia and optic atrophy, and primary hypogonadism in females. The first symptoms of the disease appear around the age of 1 year.

The well-known neuropathologic classification of ataxias by Holmes (4) includes olivopontocerebellar atrophy, spinocerebellar degeneration, and cerebellar cortical atrophy or primary parenchymatous degeneration of the cerebellum. The radiologic equivalents of these entities have been widely studied especially after the introduction of computed tomography (CT) and magnetic resonance (MR) imaging (5–10).

We analyzed the brain CT and MR findings of 17 patients with IOSCA to determine whether this clinically distinct group of patients has a uniform radiologic pattern of central nervous system involvement, and whether the CT and MR changes follow the progressive course of the disease.

Patients and Methods

We examined 16 patients with IOSCA, including 5 pairs of siblings, with CT and MR imaging in Children's Hospital, University of Helsinki, Finland, between 1988 and 1992. One patient with only an outside CT scan from 1981 was included in the study. The patients ranged in age from 1 to 29 years. Diagnosis was based on clinical presentation and family history. Extensive laboratory tests of blood,

Received September 14, 1994; accepted after revision February 22, 1995.

From the Department of Child Neurology, Children's Hospital University of Helsinki (T.K., L.V., H.P.); and the Department of Radiology, University of Texas Medical Branch at Galveston (L.M.K.).

Address reprint requests to Leena M. Ketonen, MD, PhD, Department of Radiology, University of Texas Medical Branch at Galveston, University Hospital Clinics Building, Room 2.103, Route G-09, Galveston, TX 77555.

AJNR 16:1427–1433, Aug 1995 0195-6108/95/1607–1427

TABLE 1: Neurophysiologic and imaging findings in IOSCA

Patient/Sex	Age, y, at the Time of:		Sural Nerve Conduction Velocity*, m/s	Cerebellar Cortex	Brain Stem	Spinal Cord	Small Bony Posterior Fossa	Cerebrum	Cerebellar White Matter Changes
	CT	MR							
1/F	29	29	nm	+++	+	+	++	−	p
2/M	22	22	nm	+†	−	. . .	+	−	. . .
3/F	22	24	nm	+++	−	−	−	+	a
4/F	21	21	nm	+++	+	−	++	−	a
5/F	11		. . .	−	−	. . .	−	−	. . .
		22	nm	++	++	+	++	−	a
6/M	18	19, 21	nm	+++	++	+	+	+	p
7/M	17	17, 20	nm	++	++	−	−	−	p
8/M		19	nm	++	+	+	++	−	a
9/M	16	16	nm	+	−	. . .	+	−	. . .
10/M	15	15	nm	+	−	. . .	+	−	. . .
11/F	6	. . .	. . .	−	−	. . .	−	−	. . .
12/F	3	. . .	. . .	−	−	. . .	−	−	. . .
	9	9	nm	++	+	. . .	−	−	. . .
13/F	6	. . .	32.0	+	+	. . .	−	−	. . .
14/M	2	. . .	33.0	−	−	. . .	−	−	. . .
	6	6	36.9	+	−	−	−	−	a
15/M	3	3	33.3	−	−	. . .	−	−	. . .
16/F	2	. . .	39.0	−	−	. . .	−	−	. . .
17/M	1	1	40.6	−	−	−	−	−	a

Note.—+ indicates mild atrophy; ++, moderate atrophy; +++, severe atrophy; −, no atrophy, normal; nm, nonmeasurable; p, present; and a, absent.

* Normal values > 40 m/s.

† Patient with large posterior fossa arachnoid cyst.

cerebrospinal fluid, and urine revealed no underlying metabolic abnormality. Sural nerve biopsy findings were normal in patients younger than 4.5 years of age, but degeneration of the large myelinated fibers was seen in older patients (Table 1). No mitochondrial abnormalities or abnormal storage material were observed on electron microscopy. The sensory nerve conduction measurements were made according to the method described earlier (2).

Altogether, 14 CT studies and 18 MR studies were performed. Eleven patients had both CT and MR. No formal spinal cord imaging studies were performed. CT studies were performed with contiguous 4-mm sections through the posterior fossa and 8-mm sections through the brain without intravenous contrast. The MR images were acquired either with a 1.0-T unit (nine patients) or a 0.02-T unit (eight patients). The high-field MR study included proton density–weighted and T2-weighted spin-echo images in the axial plane with a dual-echo technique (2200/22, 90/1 [repetition time/echo time/excitations]). The section thickness was 5.0 mm, and the intersection gap was 1.0 mm. T1-weighted images (500/15/1) were acquired in axial and sagittal planes, 4-mm section thickness and 0.4-mm intersection gap. The matrix size was 256 × 256, and the field of view was 23 cm in all images. No intravenous contrast was used. The low–field-strength MR studies consisted of axial 10-mm T2-weighted images (2600/130). Involuntary movements caused some degradation of the image quality in three patients and necessitated intravenous sedation of one patient. Previous CT studies were available for three patients, allowing a follow-up time of 4 to 10 years.

Images were evaluated by two experienced neuroradiologists (L.V. and L.M.K.). Cerebellar atrophy was graded visually as mild, moderate, or severe by the following criteria: *mild*, some enlarged cerebellar sulci visible, normal size of the posterior fossa cisterns; *moderate*, moderate enlargement of several sulci with enlargement of the cisterna magna and superior cerebellar cistern; and *severe*, marked enlargement of all cisterns and large fluid collections around the cerebellar hemispheres.

Brain stem atrophy was graded as mild, moderate, or severe by visually evaluating the width of the prepontine cistern, the shape of the basis pontis, and the size of the fourth ventricle. Parenchymal changes were analyzed in the T2-weighted and proton density–weighted images. The sagittal T1-weighted brain MR images allowed for evaluation of the thickness of the upper cervical cord in nine patients. Cord atrophy, when seen, was again graded from mild to moderate and severe. No axial T2-weighted images were available of the cervical cord.

Results

Posterior Fossa and Upper Cervical Cord

Cerebellar cortical atrophy was seen in 13 of the 17 patients. The cerebellar hemispheres and vermis were equally affected. Atrophy could be

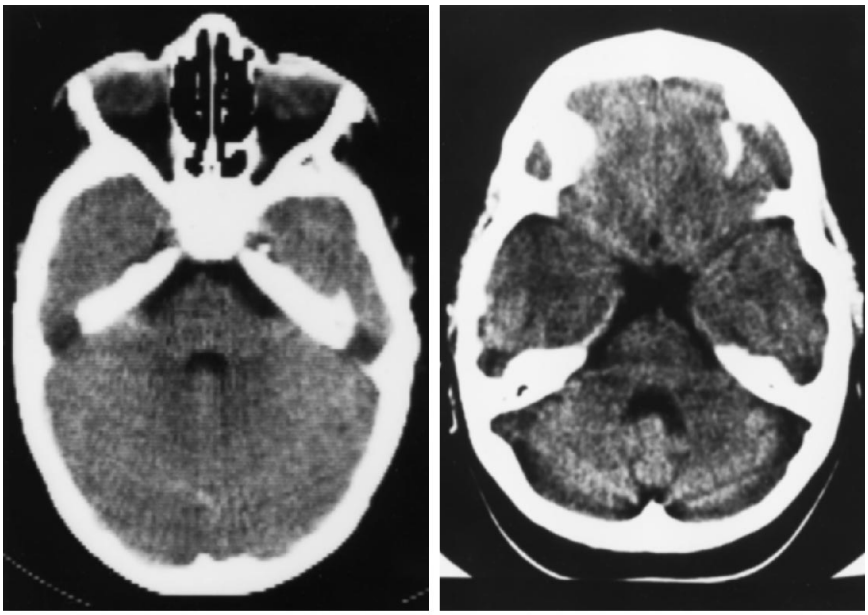

Fig 1. *A*, CT study of patient 12 at the age of 3 years shows a normal appearance of the cerebellum.

B, Follow-up study 6 years later reveals moderate cerebellar atrophy with mild widening of the fourth ventricle.

classified as mild in 5 patients, moderate in 4, and severe in 4. Table 1 shows the correlation between age and the degree of atrophy. The 3 youngest patients, 1 to 3 years of age, had no cerebellar atrophy. The first presentation of cerebellar atrophy was 4.5 years after the onset of symptoms. Severe atrophy was found in 4 of the 6 oldest patients. The 3 patients with previous CT studies for comparison all showed progression of atrophy (Fig 1). Patient 11 was examined only with CT in 1981 at the age of 6 years and had no cerebellar atrophy by that time. The finding of cerebellar atrophy also seemed to correlate with nonmeasurable nerve conduction velocities of the sural nerve.

Five of the patients had mild brain stem atrophy; moderate atrophy of the brain stem was noted in three. The fourth ventricle was of normal size in all patients with mild brain stem atrophy and enlarged in three of the four patients with moderate atrophy. The middle cerebellar peduncles were only slightly atrophic in the patients with moderate brain stem atrophy, but no flattening of the basis pontis was noted (Figs 2 and 4A). No signal changes were seen in the brain stem, but one patient had subtle hyperintensity of the left middle cerebellar peduncle in T2-weighted images. The cerebellar white matter showed patchy hyperintensity in T2-weighted images in three patients, and in one patient the dentate nuclei were also involved (Figs 3 and 4B and C). The upper spinal cord was narrow in four patients, measuring less than half of the sagittal diameter of the bony spinal canal at the level of C1–2 interspace. The cord could, however, be evaluated only in the nine patients with high-field MR studies; in others visibility was not adequate. Eight patients had abnormally small bony posterior fossae, and one patient had a large posterior fossa arachnoid cyst with small cerebellar hemispheres.

Fig 2. T1-weighted sagittal MR image (500/15/1) of patient 8. No flattening of the basis pontis is noted (*arrow*). The prepontine cistern and the fourth ventricle are slightly widened, indicating mild brain stem atrophy. There was atrophy of the upper cervical spinal cord.

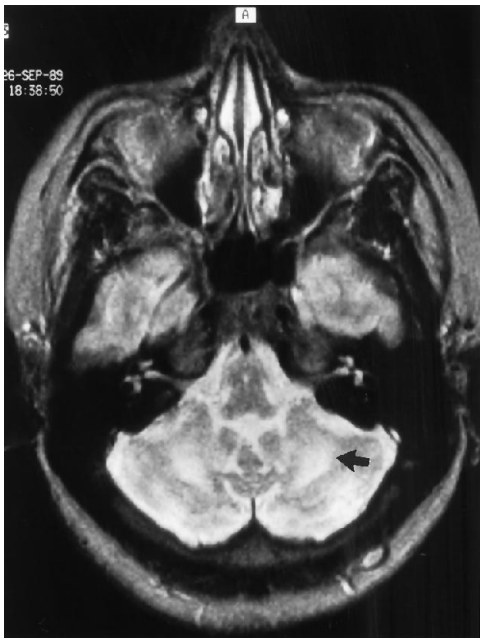

Fig 3. T2-weighted axial MR image (2200/90/1) of patient 1 shows hyperintense lesions within the cerebellar white matter (*arrow*). Cerebellar hemispheres are severely atrophic.

Supratentorial Findings

The cerebral hemispheres and basal ganglia were initially normal in all patients with no evidence of atrophy or parenchymal changes. Two patients, patients 3 and 6, were examined with either CT or MR before, during, and after a prolonged episode of status epilepticus; there were no supratentorial parenchymal changes before the acute crisis. The brain was normal during the acute phase in patient 3, but 3 weeks later a CT scan showed a right temporal hypodensity consistent with edema. An MR examination 1.5 years later revealed no signal changes, but the patient had developed mild supratentorial cortical atrophy. The MR scan of patient 6, done after several days of continuous status epilepticus, displayed multiple small hyperintense foci bilaterally in the cortical gray matter and basal ganglia. In a follow-up scan 2 months later, the changes had disappeared, but a new small hyperintense lesion was seen in an entirely new location; 1.5 years later, MR showed no parenchymal lesions, but mild cerebral atrophy was present (Fig 4D–F).

Discussion

IOSCA is a newly described recessively inherited spinocerebellar ataxia with early and severe involvement of both the peripheral and central nervous systems. Nosologically IOSCA belongs to the inherited ataxias. These include Friedreich ataxia, the early-onset cerebellar ataxias, and autosomal dominant cerebellar ataxia with different subgroups (10). Considerable overlap has been shown to exist between these clinical disorders and the neuropathologic entities of cerebellar cortical atrophy, olivopontocerebellar atrophy, and spinocerebellar atrophy, which are reflected in the imaging studies (Table 2) (7, 8).

IOSCA manifests clinically with acute or subacute onset of clumsiness in previously healthy toddlers, often in connection with minor viral infection. Ataxia, athetosis, and hypotonia with a loss of deep tendon reflexes are present in the early stage, usually between 9 and 18 months of age. Opthalmoplegia and severe sensoneural hearing loss are diagnosed by school age. Optic atrophy and sensory neuropathy are seen in adolescents, as well as primary hypogonadism in females. The mental capacity of the patients is initially unimpaired with impairment recognized at a later stage of disease. Epilepsy is a late manifestation, often presenting with a life-threatening crisis of status epilepticus and a subsequent rapid clinical deterioration. The most important pathologic finding is an early and rapidly progressive axonal neuropathy, found in a sural nerve biopsy.

In our patients the characteristic finding was a mixture of cerebellar cortical atrophy, olivopontocerebellar atrophy, and spinocerebellar atrophy. The earliest finding, cerebellar cortical atrophy, was not seen at the time of onset of symptoms but appeared some years later and progressed with the clinical disease. Follow-up studies of three patients all revealed progression of atrophic changes. Severe atrophy was seen in older patients with long-standing disease. The finding of a small bony posterior fossa suggests early involvement of the cerebellum, with subsequent failure of the bony structures to develop in a normal fashion. The neuroradiologic features of olivopontocerebellar atrophy, enlargement of the prepontine cistern, shrinkage of the middle cerebellar peduncles, and widening of the fourth ventricle, first appeared in the later stage of the disease. However, even in the most severely affected patients, flattening of the basis pontis, the imaging hallmark of olivopontocerebellar atrophy, was not seen. Savoiardo et al (6) described cerebellar paren-

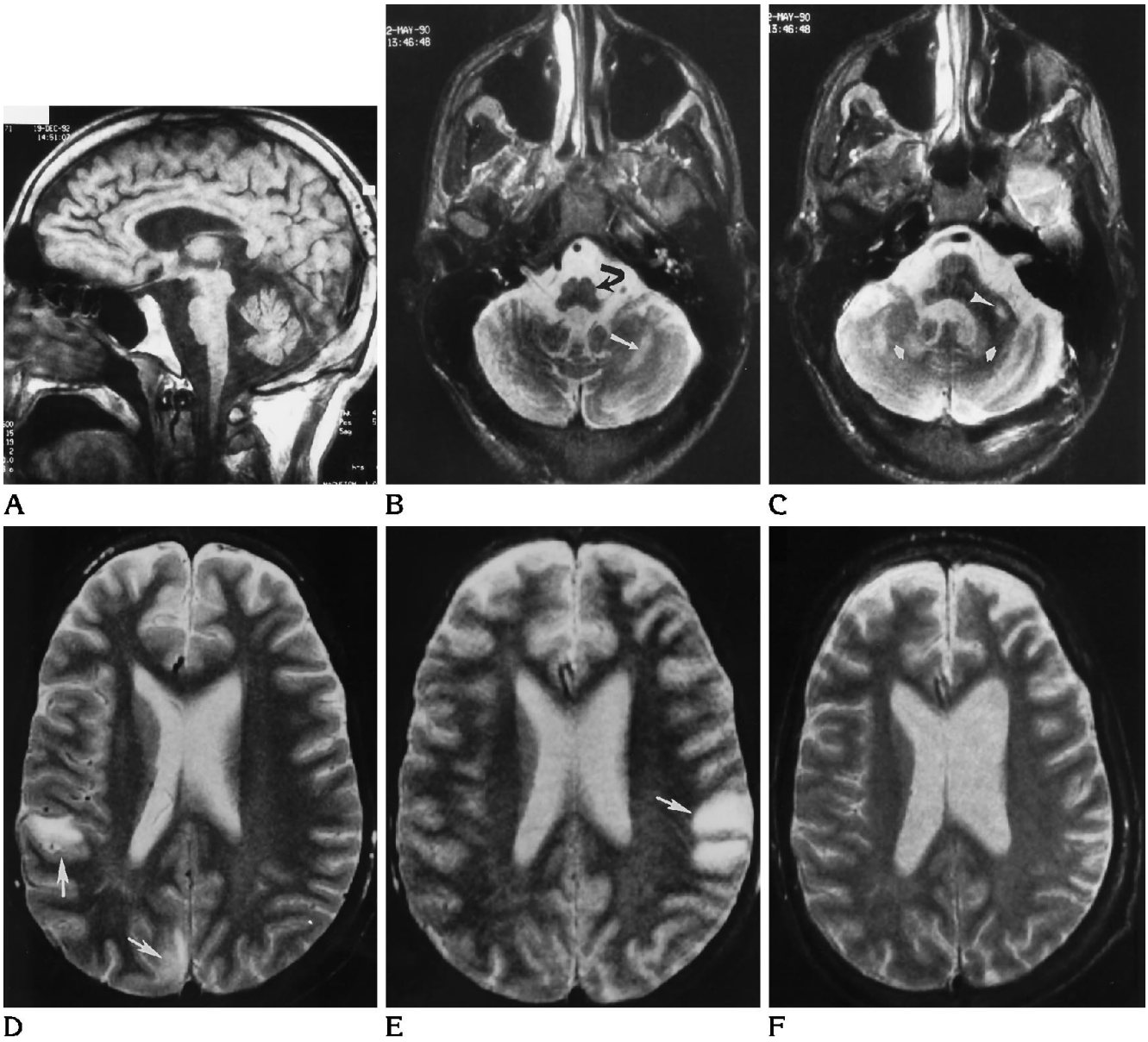

Fig 4. *A*, T1-weighted sagittal image (500/15/1) of patient 6. Atrophy of the brain stem is evident, but the shape of the belly of the pons is still preserved. There is marked widening of all posterior fossa cerebrospinal fluid spaces.

B and *C*, T2-weighted axial images (2200/90/1) through the cerebellum of the same patient reveal hyperintense lesions in cerebellar white matter (*arrow*), both dentate nuclei (*small arrows*), and the left middle cerebellar peduncle (*arrowhead*). The cerebellar atrophy is graded as severe. The inferior olivary nuclei are normal (*curved arrow*).

D, T2-weighted image of the same patient in the early stage of persistent epileptiform seizures shows two lesions in the right cerebral hemisphere (*arrows*).

E, Two weeks later, the lesions have disappeared, and a new lesion is visible in the left hemisphere (*arrow*).

F, Six months after the episode, the focal lesions have disappeared, but there is widening of the ventricles and cortical sulci consistent with atrophy.

chymal hyperintensity in T2-weighted MR images of patients with olivopontocerebellar atrophy. This finding was not confirmed by Gallucci et al (7) but was present in three of our patients, all of whom had brain stem atrophy. Although the pathologic basis of these hyperintensities is not confirmed, degeneration of Purkinje cells together with gliosis of transverse pontine fibers is a possible explanation.

Moderate atrophy of the cervical spinal cord was encountered in four severely affected patients. However, the role of spinocerebellar at-

TABLE 2: Imaging findings of hereditary ataxias

Clinical Disease	Neuropathologic Classification		
	Cerebellar cortical atrophy	Olivopontocerebellar atrophy	Spinal atrophy
IOSCA	+++	++	++(?)
Friedreich ataxia	+	−	+++
Early-onset cerebellar ataxia	+++	++	+
Autosomal dominant cerebellar ataxia type 1	+++	+++	+

Note.—+ indicates mild; ++, moderate; and +++, severe (7, 8, 11).

rophy in IOSCA still needs to be assessed, because neurophysiologic studies suggest severe, early involvement of the spinal cord. Only a small number of our patients had images of the upper cervical cord, and none underwent formal cord studies. Signal changes in the spinal cord, described in Friedreich ataxia (11), could not be evaluated in this study and need further investigation with high-quality T2-weighted axial images. Early loss of deep-tendon reflexes and axonal sensory neuropathy are common features in Friedreich ataxia and IOSCA (2, 12). Myocardial involvement, which is common in Friedreich ataxia, is not seen in IOSCA. Spinal cord atrophy is the most prominent imaging feature in Friedreich ataxia. The role of cerebellar atrophy in Friedreich ataxia has been discussed in recent papers (13), and controversy exist over this issue. However, neuropathologic studies have shown either absence of atrophic changes or only mild atrophy (14).

The early-onset cerebellar ataxias are a group of progressive ataxias with onset before the age of 25 years. They are clinically distinguished from Friedreich ataxia and IOSCA by preservation of deep-tendon reflexes (15, 16). Genetic heterogeneity has been suspected in patients with early-onset cerebellar ataxia because of the variable clinical course (17). Cerebellar cortical atrophy is frequently seen in patients with early-onset cerebellar ataxia. Atrophy of the cervical spinal cord and medulla oblongata have also been described (8, 9, 18). The autosomal dominant cerebellar ataxias are a heterogenous group of usually dominantly inherited diseases, which mainly occur in adulthood. Genetic heterogeneity has been shown with linkage analysis in autosomal dominant cerebellar ataxia type 1 (19). Neuropathy in autosomal dominant cerebellar ataxia is less severe than in IOSCA. The morphologic changes of autosomal dominant cerebellar ataxia include cerebellar atrophy with various forms of additional findings from spinal cord atrophy to olivopontocerebellar atrophy (8, 9).

Transient parenchymal changes after prolonged status epilepticus in our two patients are similar to the findings described after a focal epileptic seizure (20–22), in hypertensive encephalopathy (23), in an attack of acute intermittent porphyria with seizures and hallucinations (24), and in mitochondrial encephalopathies, especially in MELAS (mitochondrial encephalopathy with lactic acidosis and stroke-like episodes) (25). The pathophysiology of such radiologic abnormalities is poorly understood. The positron emission tomographic finding of an ictal hypermetabolic neuronal state and hyperperfusion in the region of epileptic focus is perhaps attributable to tissue hypoxia, lactic acidosis, and/or dysautoregulation of cerebral blood flow (26). Breakdown of the blood-brain barrier has been noted in clinical and experimentally induced prolonged seizures (26). In our patients, the transient CT and MR changes appeared after prolonged seizures, maybe induced by the unknown underlying metabolic defect.

In conclusion, the CT and MR findings of patients with IOSCA again show the known overlap of cerebellar cortical atrophy, olivopontocerebellar atrophy, and spinocerebellar atrophy in hereditary ataxias, confirming that imaging studies cannot be used for definite diagnosis of these diseases. However, in IOSCA the atrophic changes were seen earlier than in many other clinically related conditions, and there was a correlation between the progression of the clinical symptoms, the increasing severity of cerebellar atrophy, and the appearance of olivopontocerebellar atrophy–type changes. Our findings again support the concept that the neuropathologic subgroups are not separate entities but rather variations of a degenerative process, which can have different causes.

References

1. Koskinen T, Santavuori P, Sainio K, Lappi M, Kallio A-K, Pihko H. Infantile onset spinocerebellar ataxia with sensory neuropathy: a new inherited disease. *J Neurol Sci* 1994;121:50–56

2. Koskinen T, Sainio K, Rapola J, Pihko H, Paetau A. Sensory neuropathy in infantile onset spinocerebellar ataxia (IOSCA). *Muscle Nerve* 1994;17:509–515
3. Nikali K, Suomalainen A, Terwillinger J, Koskinen T, Weissenbach J, Peltonen L. Random search for shared chromosmal regions in four affected individuals: the assignment of a new ataxia locus. *Am J Hum Genet* 1995;56:1088–1095
4. Holmes G. An attempt to classify cerebellar disease, with a note on Marie's hereditary cerebellar ataxia. *Brain* 1907;30:545–567
5. Wittkamper A, Wessel K, Bruckmann H. CT in autosomal dominant and idiopathic cerebellar ataxia. *Neuroradiology* 1993;35: 520–524
6. Savoiardo M, Strada L, Girotti F, et al. Olivopontocerebellar atrophy: MR diagnosis and relationship to multisystem atrophy. *Radiology* 1990;174:693–696
7. Galucci M, Splendiani A, Bozzao A, et al. MR imaging of degenerative disorders of brainstem and cerebellum. *Magn Reson Imaging* 1990;8:117–122
8. Wullner U, Klockgether T, Petersen D, Naegele T, Dichgans J. Magnetic resonance imaging in hereditary and idiopathic ataxia. *Neurology* 1993;43:318–325
9. Klockgether T, Wullner U, Dichgans J, et al. Clinical and imaging correlations in inherited ataxias. *Adv Neurol* 1993;61:77–96
10. Harding AE. Classification of the hereditary ataxias and paraplegias. *Lancet* 1983;i:1151–1154
11. Mascalchi M, Salvi F, Piacentini S, Bartolozzi S. Friedreich's ataxia: MR findings involving the cervical portion of the spinal cord. *AJR Am J Roentgenol* 1994;163:187–191
12. Santoro L, Perretti A, Crisci C, et al. Electrophysiological and histological follow-up study in 15 Friedreich's ataxia patients. *Muscle Nerve* 1990;13:536–540
13. Junck L, Gilman S, Gebarski S, Koeppe R, Kluin K, Markel D. Structural and functional brain imaging in Friedreich's ataxia. *Arch Neurol* 1994;51:349–355
14. Openheimer D. Brain lesions in Friedreich's ataxia. *Can J Neurol Sci* 1979;2:173–176
15. Plaitakis A, Katoh S, Huang YP. Clinical and radiological features of cerebellar degeneration. In: Plaitakis A, ed. *Cerebellar Degenerations: Clinical Neurobiology*. Boston: Kluwer Academic Publishers, 1992:305–365
16. Harding AE. Early onset cerebellar atrophy with retained tendon reflexes: a clinical and genetic study of a disorder different from Friedreich's ataxia. *J Neurol Neurosurg Psychiatry* 1981;44:503–508
17. Filla A, De Michele G, Calvacanti F, et al. Clinical and genetic heterogeneity in early onset cerebellar ataxia with retained tendon reflexes. *J Neurol Neurosurg Psychiatry* 1990;53:667–670
18. Klockgether T, Petersen D, Grodd W, Dichgans J. Early onset cerebellar ataxia with retained tendon reflexes. Clinical, electrophysiological and MRI observations in comparison to Friedreich's ataxia. *Brain* 1991;114:1559–1573
19. Khati C, Stevanin G, Durr A, et al. Genetic heterogeneity of autosomal dominant cerebellar ataxia type 1. *Neurology* 1993;43: 1131–1137
20. Dillon W, Brant-Zawadzki M, Sherry RG. Transient computed tomographic abnormalities after focal seizures. *AJNR Am J Neuroradiol* 1984;5:107–109
21. Jayakumar PN, Taly AB, Mohan PK. Transient computerized tomographic (CT) abnormalities following partial seizures. *Acta Neurol Scand* 1985;72:26–29
22. Kramer RE, Luders H, Lesser RP, et al. Transient focal abnormalities of neuroimaging studies during focal status epilepticus. *Epilepsia* 1987;28:528–532
23. Hauser RA, Lacey M, Knight MR. Hypertensive encephalopathy. Magnetic resonance imaging demonstration of reversible cortical and white matter lesions. *Arch Neurol* 1988;45:1078–1083
24. King PH, Bragdon AC. MRI reveals multiple reversible cerebral lesions in an attack of acute intermittent porphyria. *Neurology* 1991;41:1300–1302
25. Abe K, Inui T, Hirono N, Mezaki T, Kobayashi Y, Kameyama M. Fluctuating MR images with mitochondrial encephalopathy, lactic acidosis, stroke-like syndrome (MELAS). *Neuroradiology* 1990; 32:77
26. Engel J, Kuhl DE, Phelps ME, Rausch R, Nuwer M. Local cerebral metabolism during partial seizures. *Neurology* 1983;33:400–413
27. Nitsch C, Klatzo I. Regional patterns of blood-brain barrier breakdown during epileptiform seizures induced by various convulsive agents. *J Neurol Sci* 1983;59:305–322